ASM Sc. J., 14, Special Issue 1, 2021 for ICSTSS2018, 169-174

A Physicochemical Study of Samarium Oxide-Based Catalyst for CO_2 Hydrogenation Reaction: Effect of Loadings

Salmiah Jamal Mat Rosid[1]*, Susilawati Toemen[2], Wan Azelee Wan Abu Bakar[2], Nurulhuda Mohammad Yusoff[1], Ahmad Zamani Ab Halim[3] and Wan Nur Aini Wan Mokhtar[4]

[1]*Unisza Science and Medicine Foundation Centre, Universiti Sultan Zainal Abidin, Gong Badak Campus, 21300 Kuala Nerus, Terengganu, Malaysia*

[2]*Department of Chemistry, Faculty of Science, Universiti Teknologi Malaysia, 81310 UTM Skudai, Johor, Malaysia*

[3]*Faculty of Industrial Sciences & Technology, Universiti Malaysia Pahang, 26300 Gambang, Kuantan, Pahang, Malaysia*

[4]*Centre for Advanced Materials and Renewable Resources, Faculty of Science and Technology, Universiti Kebangsaan Malaysia, 43600 Bangi, Selangor, Malaysia*

Catalytic reaction has been widely explored for converting carbon dioxide (CO_2) to methane (CH_4). A series of samarium oxide-based catalyst was screened, while the potential Ru/Mn/Sm (5:35:60)/Al_2O_3 was further analysed due to the highest CO_2 conversion (92.52%) yielded at 250 ^oC reaction temperature via wetness impregnation method. The catalytic activity using a home-built reactor-FTIR a ratio of H_2/CO_2 4:1 displayed that the CO_2 conversion increased gradually due to the effectiveness of catalysts to increase hydrogenation activity. Therefore, the base loading was varied between 55% and 65% to observe the active species that contributed to higher catalytic activity. The XRD analysis revealed the presence of samarium oxide (Sm_2O_3) and manganese (II) oxide (MnO_2) that served as active species to enhance the catalytic activity at 60% Sm-based loading. The existence of rhombohedral α-Al_2O_3 at 55% and 65% Sm-based loading appeared to lower the catalytic activity of the catalyst due to nucleation and crystallite growth process. Next, FESEM unearth a spherical shape with 120-130 nm particle sizes. The EDX analysis displayed that all active elements were present on the catalyst surface. As conclusion, Sm-based loading did had an impact on catalytic activity and physicochemical properties.

Keywords: hydrogenation; catalyst; CO_2; methanation; samarium

I. INTRODUCTION

Catalytic methanation reaction has been widely explored for conversion of CO_2 to CH_4 gas by reducing emission of greenhouse gases using metal oxide. The widely used conventional metal oxide catalysts are nickel, cobalt, manganese, copper (Zamani *et al*., 2014), and iron (Vedrine, 2017). Metal oxide catalysts tend to deactivate after several hours due to carbon formation. This problem, nonetheless, can be addressed by using a noble metal to function as a dopant mix with metal oxide catalyst. Some common noble metals applied are rhodium, ruthenium, platinum, and iridium, which can generate high CO_2/H_2 methanation performance, and less sensitivity towards coke deposition. Nevertheless, from the practical viewpoint, noble metals are costly and not to avail in abundance. Hence, an alternative is proposed by incorporating dopants and co-dopants into noble metal to slash cost. Chunhui *et al.* (2010), for instance, incorporated samarium into Ba-Ru-K/AC (active carbon) to enhance catalytic activity and stability.

From our prior study, samarium was selected as the base and ruthenium as the co-dopant catalyst to achieve higher CO_2 conversion (Rosid *et al.*, 2013). The results showed that

*Corresponding author's e-mail: salmiahjamal@unisza.edu.my

Ru/Mn/Sm (5:35:60)/Al_2O_3 can be a potential catalyst for CO_2 methanation reaction as it gave 100% CO_2 conversion with 93.46% CH_4 formation (Rosid *et al.*, 2013). High CO_2 methanation was recorded only at higher reaction temperature of 400 °C. Hence, this paper further probed into the catalyst to achieve high CO_2 methanation at lower temperature. The catalyst was optimised to determine the effects of samarium-based loading and calcination temperature. Next, the catalysts were characterised using XRD, FESEM, EDX, and BET analyses to observe the physicochemical properties based on the effect of loadings.

II. MATERIALS AND METHODS

A. Preparation of Catalyst

The catalyst was prepared by dissolving 5 g of samarium oxide hexahydrate with 5 mL of distilled water with 60% ratio. Next, manganese (II) nitrate and ruthenium (III) chloride were added at ratios 35% and 5%, respectively. The mixed solution was doped with alumina bead and stirred for about 30 minutes prior to aging in oven at 90 °C for 24 hours. After that, the catalysts were calcined at 400 °C, followed by 700 °C, 800 °C, 900 °C, 1000 °C, and 1100 °C. These steps were repeated for various ratios, as summarised in Table 1.

Table 1. Prepation of samarium oxide catalyst by different ratios

Catalysts	Ratio, %
Sm	100
Mn/Sm	40:60
Mn/Sm	30:70
Mn/Sm	20:80
Mn/Sm	10:90
Ru/Mn/Sm	5:40:55
Ru/Mn/Sm	5:35:60
Ru/Mn/Sm	5:30:65
Ru/Mn/Sm	5:25:70
Ru/Mn/Sm	5:20:75
Ru/Mn/Sm	5:15:80
Ru/Mn/Sm	5:10:85

B. Catalytic Screening by Fourier Transform Infrared (FTIR)

Both CO_2 and H_2 gases were mixed in a mixture cylinder with a molar ratio of 1:4 and continuously flowed through the prepared catalyst. Next, the mixture of gases was heated in isothermal tube furnace at a flow rate of 50.00 cm^3/min for 20 minutes. The calibration was run using in-situ FTIR at room temperature, while the catalytic reaction temperature was fixed between 60 °C and 400 °C with increment of 5 °C/min. Figure 1 illustrates the home-built micro reactor.

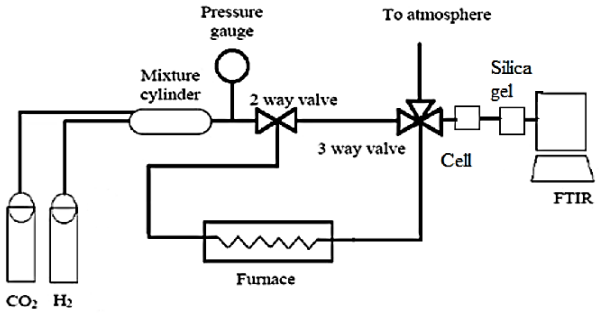

Figure 1. Schematic illustration of home-built micro reactor setup coupled with FTIR

C. Methane Measurement via Gas Chromatography

The products obtained from the irradiated temperature range were CH_4 and H_2O. Presence of methane was determined by using gas chromatography Hewlett Packard 6890 Series with column ultra 1. Carrier Helium gas with a rate flow 20 ml/min at 75 kPa was applied. The starting temperature was set at 40 °C for 7 minutes, whereas the injection and detection temperatures were 150 °C and 310 °C, respectively.

D. Characterisation of Catalyst

The XRD analysis was performed by using Crystalloflex D5000 Diffractometer with CuKα radiation (λ=1.54060A). As for FESEM-EDX analysis, a 15 kV Zeiss Supra 35 VP FESEM coupled with EDX analyser was employed to scan the sample under 25 kV. Next, BET analysis was performed using Micromeritics ASAP 2010 after degassing nitrogen gas at 120 °C with a flow rate of 50 µL/min.

III. RESULTS AND DISCUSSION

A. Catalytic Activity of Catalyst

The initial screening of monometallic oxide, Sm, calcined at 400 °C gave only 15% of CO_2 conversion. To improve the performance of catalyst, manganese was incorporated as a dopant with various ratios; Mn/Sm (40:60)/Al_2O_3, Mn/Sm

(30:70)/Al_2O_3, Mn/Sm (20:80)/Al_2O_3, and Mn/Sm (10:90)/Al_2O_3. Figure 2 portrays the trend of catalytic activity. The addition of manganese resulted in insignificant effect on the catalyst performance, when compared with the monometallic catalyst. The highest CO_2 conversion at 23% was observed at 400 °C reaction temperature.

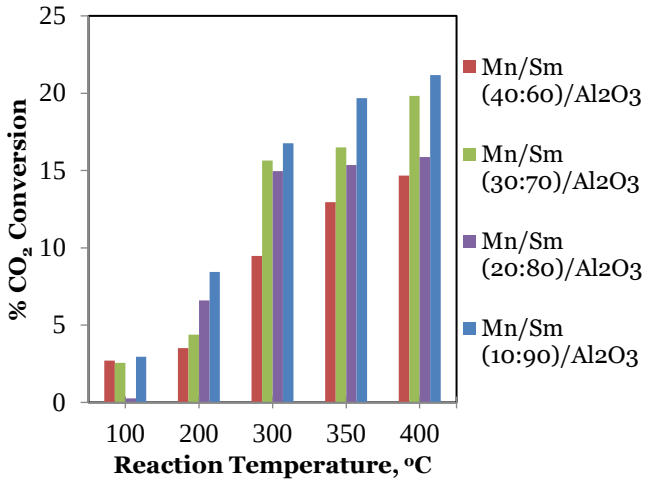

Figure 2. CO_2 conversion over Mn/Sm with different ratios calcined at 400 °C

Low CO_2 conversion of monometallic and bimetallic oxide catalysts steered to the trimetallic oxide catalyst with ruthenium as the co-dopant. The resulting outcomes are tabulated in Table 2. It was noted that Ru/Mn/Sm (5:35:60)/Al_2O_3 catalyst calcined at 400 °C attained 96% of CO_2 conversion at the maximum reaction temperature of 400 °C, while the conversion for all prepared trimetallic catalysts exceeded 50%.

Table 2. Conversion of CO_2 by Ru/Mn/Sm/Al_2O_3 catalyst calcined at 400 °C

Ratio, %	Reaction Temperature (°C)					
	100	200	250	300	350	400
	% Conversion of CO_2					
5:40:55	2.3	13.2	31.2	40.3	62.4	68.4
5:35:60	5.3	12.0	25.6	48.9	79.7	96.2
5:30:65	2.1	12.3	26.4	46.4	69.5	88.3
5:25:70	2.1	20.3	27.6	65.4	66.3	82.1
5:20:75	5.6	33.4	36.4	50.4	63.2	79.4
5:15:80	8.9	13.4	20.3	41.2	49.7	69.3
5:10:85	4.3	19.4	23.2	43.2	46.7	54.3

The findings indicated that the addition of ruthenium into Al_2O_3 support enhanced the activity of the catalyst, which is in line with that reported by Vedrine (2017). This was also due to the increased manganese ratio in the catalysts, as manganese served as an excellent reducing agent that enhanced the reduction of CO_2 to methane (Rosid *et al.*, 2013). Increment of the manganese ratio to 40% decreased the CO_2 conversion to 68%, which is ascribed to active site blockage owing to the uneven distribution of manganese oxide on the catalyst surface.

The highest CO_2 conversion attained only at 400 °C reaction temperature is impractical for industry purpose. The minimum requirement operating temperature for industry is below 250 °C reaction temperature. Hence, Ru/Mn/Sm(5:35:60)/Al_2O_3 catalyst was furthered calcined up to 1100 °C. Table 3 presents the conversion of CO_2 with Ru/Mn/Sm (5:35:60)/Al_2O_3 calcined at varied temperatures.

Table 3. Conversion of CO_2 by Ru/Mn/Sm (5:35:60)/Al_2O_3 calcined at different temperatures

C. T * (°C)	Reaction Temperature (°C)					
	100	200	250	300	350	400
	% Conversion of CO_2					
400	5.3	12.0	25.7	48.9	79.6	96.3
700	3.4	14.4	34.4	61.0	85.3	96.7
900	8.9	21.3	45.6	70.3	80.6	91.5
1000	10.3	65.5	92.5	95.5	98.8	100.0
1100	13.4	70.5	86.7	96.7	98.0	99.3

*Calcination Temperature

Table 3 reveals that increment of calcination temperature increased the percentage of CO_2 conversion. This phenomenon is attributable to Sm^{3+} ions that stabilised the lattice and increased oxygen vacancies at higher calcination temperature, as suggested by Frontera *et al.* (2017), although the density of active sites on the surface had decreased (Hashimoto *et al.*, 2013). Similarly, Gil *et al.* (2004) reported that the presence of single manganese oxide affected both the calcination temperature and the structure of the catalyst. The CO_2 conversion slightly decreased at 1100 °C due to atom migration sintering that led to loss of active surface area, similarly observed by Rostrup *et al.* (2007). Hence, catalyst calcined at 1000 °C gave the best outcome with above 92% of CO_2 conversion at 250 °C reaction temperature.

B. Characterisation of Catalyst

The Ru/Mn/Sm)/Al_2O_3 catalyst calcined at 1000 °C was characterised to determine its physicochemical properties.

1. X-ray Diffraction (XRD) Analysis

The XRD analysis was performed at different base loadings (55%, 60%, and 65%) (see Figure 3). All the diffraction patterns represented polycrystalline peaks on the surface of the catalyst. Most of the diffractogram peaks were dominated by Al_2O_3 on the cubic phase, hence verifying the presence of alumina phase as support.

Figure 3 illustrates peaks of Sm_2O_3 (cubic), RuO_2 (tetragonal), MnO_2 (tetragonal), Al_2O_3 (cubic), and corundum Al_2O_3 (rhombohedral) at 55% and 65% samarium loading. The intense peaks of the cubic phase Al_2O_3 were assigned to 66.85° (I_{100}), 45.79° (I_{100}), 37.21° (I_{90}), 39.42° (I_{50}), and 60.76° (I_{30}). The peaks of RuO_2 were tetragonal at 2θ values of 28.08° (I_{100}), 35.09° (I_{77}), and 54.53° (I_{45}). The tetragonal phase of RuO_2 was thermally stable and did not change upon exposure to higher temperatures. The tetragonal MnO_2 was overlapping at *2θ* values of 36.99° (I_{100}), 56.40° (I_{80}), and 42.82° (I_{70}). The peaks of Sm_2O_3 with cubic phase were assigned at *2θ* values of 27.88° (I_{100}), 32.31° (I_{50}), and 45.36° (I_{45}). Peaks dominated by alumina rhombohedral phase were noted at 2θ values of 35.122° (I_{100}), 43.317° (I_{96}), 57.469° (I_{91}), 25.583° (I_{68}), and 52.534 (I_{47}). Lours *et al.* (1998) reported rhombohedral of Al_2O_3 at calcination temperature exceeding 880 °C. The rhombohedral α-Al_2O_3 attained a stable phase through the nucleation and the crystallite growth processes. Thus, it increased the particle size that reduced the surface area (Miyake *et al.*, 2018), thereby decreasing catalytic activity.

In comparison to the diffractogram for 60% ratio, only Al_2O_3 cubic, Sm_2O_3 cubic, and MnO_2 tetragonal phases were detected. The low intensity of MnO_2 in the diffractogram signified the amorphous properties of the product. Besides, no peak was noted for corundum Al_2O_3 in the diffractogram of 60 wt% of Sm loading. The corundum Al_2O_3 was considered as inhibitor species in this study as it affected the catalytic activity of Ru/Mn/Sm/Al_2O_3 catalyst.

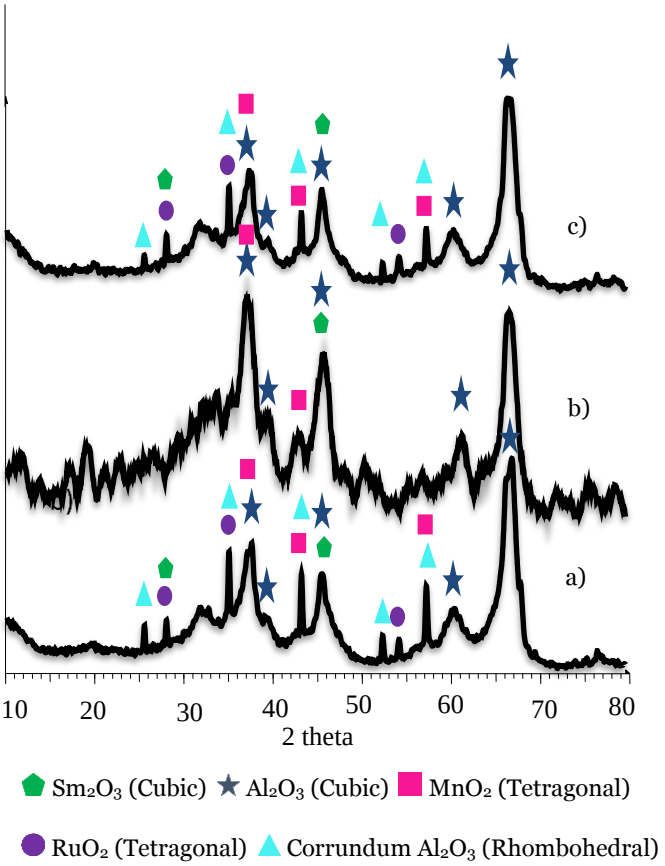

Figure 3. Diffractogram of Ru/Mn/Sm (5:35:60)/Al_2O_3 catalyst with different base loadings; a) 55%, b) 60%, and c) 65% calcined at 1000 °C

2. Field Emission Scanning Electron Microscopy (FESEM) analysis

The morphology of Ru/Mn/Sm/Al_2O_3 catalyst was determined using FESEM analysis with 55%, 60%, and 65% base loadings (see Figure 4). The magnification used was 50000X and the micrograph revealed no significant changes in their morphology.

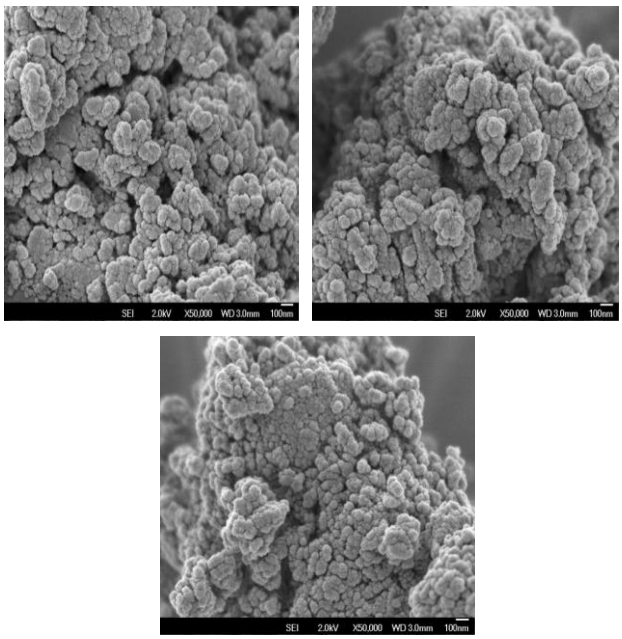

Figure. 4. Morphology of Ru/Mn/Sm /Al_2O_3 catalyst for different base loadings; a) 55%, b) 60%, and c) 65% with 50000x magnification, scale bar 100 nm, and calcined at 1000 ^oC

The micrograph demonstrates the aggregated of small spherical particle at 55 wt% of Sm loading. The particles become agglomerated as the loading was increased to 65 wt%. This is attributable for the decrease noted in the catalytic activity to 88.3% for Ru/Mn/Sm (5:30:65)/Al_2O_3 catalyst. The micrograph displayed that the catalyst at 60% had many pores that might have assisted in the CO_2 methanation activity by giving 100% CO_2 conversion at this ratio loading. The average particle size ranged at 120-130 nm, which is in accordance with XRD diffractogram that exhibited broad and polycrystalline peak as an indicator of amorphous properties.

3. Energy Dispersive X-ray (EDX) Analysis

The EDX analysis offers significant information in identifying the proportion of element on sample surface and catalyst composition that was successfully coated with support. The EDX analysis (see Table 4) revealed that the atomic ratio of Sm, Mn, and Ru was less than 1.00%. This may reflect the presence of Sm, Ru, and Mn in high porosity alumina beads, as reported by Zhuang et al. (1991). Nonetheless, when the base loading increased to 60%, the atomic ratio of each element displayed increment, except Ru. Simultaneously, when consumption was increased to 65%, the composition of Sm and Mn elements slightly reduced, except for Ru. This observation is in agreement with XRD results, which signifies the appearance of RuO_2 peak at 65%.

Table 4. Elemental composition from EDX analysis for Ru/Mn/Sm/Al_2O_3 catalyst calcined at 1000 ^oC with 55%, 60%, and 65% base loadings

Based loading, %	Atomic ratio (%)				
	Al	O	Sm	Ru	Mn
55	32.52	52.85	0.58	0.77	0.36
60	34.56	53.11	0.72	0.37	0.79
65	40.78	48.12	0.79	0.54	0.64

4. Nitrogen Adsorption (NA) Analysis

The structural properties of Ru/Mn/Sm/Al_2O_3 catalyst at various base loadings are summarised in Table 5. The reduction noted in BET surface area for catalyst at 65% base loading indicated the clogging and agglomeration of metal oxide particles. The diameter of the pores increased with higher base loadings, thus decreasing the pore volume on the catalyst surface. This finding is in line with the outcome retrieved from FESEM analysis (see Figure 4), which revealed the agglomerated particles at 65 wt% of Sm loading.

Table 5. Structural properties of Ru/Mn/Sm/Al_2O_3 catalyst at different base loadings

Catalyst	Based Loading, %	S_{BET} (m^2/g)	Pore Diameter (nm)	Pore Volume (cm^3/g)
Ru/Mn/Sm /Al_2O_3	55	99.47	136.88	0.34
	60	41.36	207.28	0.21
	65	27.43	247.05	0.17

IV. CONCLUSION

The trimetallic catalyst, Ru/Mn/Sm (5:35:60)/Al_2O_3, emerged as a potential catalyst as it resulted in above 92% of CO_2 conversion at 250 ^oC reaction temperature. The higher catalytic activity of Ru/Mn/Sm (5:35:60)/Al_2O_3 calcined at 1000 ^oC had been due to active species Sm_2O_3 and MnO_2, which was observed in the XRD analysis. At 60% base loading, aggregated and agglomerated particle with 41 m^2/g BET surface area was recorded. The EDX analysis verified the presence of active species and the composition of ruthenium on the catalyst surface.

V. ACKNOWLEDGEMENT

This research was supported by Universiti Sultan Zainal Abidin for human capital, Universiti Teknologi Malaysia for GUP grant vote 13H34, and FRGS vote no 5F076 for financial support.

VI. REFERENCES

Chunhui, Z, Yifeng, Z & Huazhang, L 2010, 'Effect of samarium on methanation resistance of activated carbon supported ruthenium catalyst for ammonia synthesis', Journal of Rare Earths, vol. 28, pp. 552-555.

Frontera, P, Macario, A. Ferraro, M & Antonucei, P 2017, 'Supported catalysts for CO_2 methanation: a review', Catalysts, vol. 7, no. 59, pp. 1.28.

Gil, A, Gandia, LM & Korili, SA 2004, 'Effect of the temperature of calcination on the catalytic performance of manganese and samarium-manganese based oxides in the complete oxidation of acetone', Applied Catalysis A: General, vol. 274, pp. 229-235.

Hashimoto, K, Kumagai, N, Izumiya, K, Takano, H, Zabinski, PR, El-moneim, AA, Yamasaki, M, Kato, Z, Akiyama, E & Hazabaki, H 2013, 'The use of renewable energy in the form of methane via electrolytic hydrogen generation', Archieves of Metallurgy and Materials, vol. 58, no. 1, pp. 231-239.

Lours, P, Alexis, J & Bernhart, G 1998, 'Oxidation resistance of ODS alloy PM2000 from 880°C to 1400°C', Journal of Materials Science Letters, vol. 17, pp. 1089-1093.

Miyake, K, Hirata, Y, Shimonosono, T & Sameshima S 2018, 'The effect of particle shape on sintering behavior and compressive strength of porous alumina', Materials, vol. 11, pp. 1137.

Rosid, SJM, Abu Bakar, WAW, & Ali R 2013, 'Methanation reaction over samarium oxide based catalysts', Malaysian Journal of Fundamental and Applied Sciences, vol. 9, no. 1, pp. 28-34.

Rostrup-Niclsen, JR, Pedersen, K & Sehested, J 2007, 'High temperature methanation sintering and structure sensitivity', Applied Catalysis A: General, vol. 330, pp. 134-138.

Vedrine, JC 2017, 'Heterogeneous catalysis on metal oxides', Catalysts, vol. 7, pp. 341.

Yaccato, K, Carhart,R, Hagemeyer, A, Lesik, A, Strasser, P, Volpe, FA, Trner, HJr, Weinberg, H, Grasselli, KR & Brooks, C 2005, 'Competitive CO and CO_2 methanation over supported noble metal catalysts in high throughput scanning mass spectrometer', Applied Catalysis A: General, vol. 296, pp. 30-48.

Zamani, AH, Ali, R & Abu Bakar WAW 2014, 'The investigation of $Ru/Mn/Cu–Al_2O_3$ oxide catalysts for CO_2/H_2 methanation in natural gas', Journal of the Taiwan Institute of Chemical Engineers, vol. 45, no. 1, pp. 143-152.

Zhuang, Q, Qin, Y & Chang, L 1991, 'Promoting effect of cerium oxide in supported nickel catalyst for hydrocarbon steam-reforming', Applied Catalyst, vol. 70, no. 1, pp. 1-8.